ELLIPTICAL RING MICROSTRIP ANTENNA WITH CIRCULAR POLARIZATION

Mitsuo TAGUCHI, Seiji OHTSU, Shigeru EGASHIRA* and Kazumasa TANAKA
Dept. of Electrical Eng. & Computer Science, Nagasaki University,
1-14 Bunkyo-machi, Nagasaki-shi, 852, Japan
*Dept. of Electronics, Saga University, Honjo-machi, Saga-shi, 840, Japan

1. Introduction

The elliptical ring microstrip antenna with a circular slot on its center is numerically analyzed and its characteristics is compared with that of the elliptical patch antenna. In the numerical analysis, the electromagnetic fields in the dielectric are expanded in terms of the Bessel functions and trigonometric functions. The fields are determined so as to satisfy the impedance boundary conditions on the apertures of inner and outer edge of antenna in the least squares sense.

2. Theory

Fig.1 shows an elliptical ring microstrip antenna. The outer edge of ring is an ellipse with semimajor axis a_0 and semiminor axis b_0, and the inner edge of it is a circle with radius a_1. The antenna is excited on the outer edge at $\phi_0=45°$ from the semimajor axis by a coaxial line through the dielectric substrate.

The thickness of the dielectric substrate is chosen to be much smaller than a wavelength in the dielectic. Then the fields in the dielectric do not vary with respect to z and the Maxwell's equations are reduced to the Helmholtz equation for the z component E_z of electric field. In the cylindrical coordinates (r, ϕ, z), the solution of the Helmholtz equaiton is assumed by a truncated sammation of E_{zn}.

$$E_z=\sum_{n=1}^{N} E_{zn}, \quad E_{zn}=\{A_nJ_n(k_1r)+B_nN_n(k_1r)\}\cos(n\phi)+\{C_nJ_n(k_1r)+D_nN_n(k_1r)\}\sin(n\phi) \tag{1}$$

where J_n and N_n are Bessel and Neumann functions of the order n, respectively, and A_n, B_n, C_n, and D_n, $n=1, 2, \ldots, N$ are unknown coefficients to be determined from the boundary conditions on the antenna apertures. We denote by H_v and H_ϕ the v component in the elliptical coordinates and ϕ component in the cylindrical coordinates of magnetic field, respectively. Then the boundary conditions on the antenna apertures are expressed as follows[1].

In the inner aperture $r=a_1$

$$H_\phi=\sum_{n=1}^{N} E_{zn}y_{sn}^{1}, \tag{2a}$$

and in the outer aperture $u=u_0$

$$-H_v=K_z+\sum_{n=1}^{N} E_{zn}y_{sn}^{0}, \tag{2b}$$

where K_z is the current maintained by the coaxial line at the feeding point:

$$K_z(v)=\frac{I_0\delta(v-v_0)}{c(\cosh^2u_0-\cos^2v_0)^{1/2}} \tag{3}$$

where I_0 is the total current at the feeding point, and y_{sn}^0 and y_{sn}^1 are the surface admittances of the order n as seen from the outer elliptical aperture bounded by $u=u_0$ and $-d\leqq z\leqq 0$ and the inner cylindrical aperture at $r=a_1$ and $-d\leqq z\leqq 0$. The surface admittances take into acount the effect of radiation and the fringe field. Since we treat the case the outer ellipse is almost a circle, the expression of the surface admittances of circular patch antenna with radii a_0 and a_1 are used[2].

On applying the boundary condition (2a), we obtain the expressions of the coefficients B_n and D_n in terms of A_n and C_n, respectively. Next we determine the coefficients A_n and C_n so that the electromagnetic fields satisfy the boundary condition (2b) in the least squares sense:

$$F=\int_0^{2\pi} | H_v + K_z + \sum_{n=1}^{N} E_{zn} y_{sn}^0 |^2 dv' \rightarrow \text{minimum} \tag{4}$$

This equation is reduced to the set of linear equations for A_n and C_n[3]. The radiation field can be calculated from the aperture electric field distributions.

3. Numerical results

First, we examined the convergence of the coefficients $\{A_n\}$ and $\{C_n\}$ and the frequency f_0 at the circular polarization as the number of mode in the electromagnetic field is increased from 4 to 16. The magnitude of coefficients of more than third order are much smaller than that of lower order, and the variation of coefficients and f_0 are within 0.02%. This is because the elliptical edge of the antenna is almost a circle and the fundamental mode is excited in this antenna. Therefore N is fixed to be 4 in the calculation of characteristics.

Fig. 2 shows the frequency characteristics of axial ratio for b_0/a_0=0.97. Fig. 3 shows the optimum axial ratio and its frequency f_0 as a function of a_1. f_0 becomes lower as a_1 becomes larger. However, f_0 does not depend on the value of b_0/a_0. As b_0/a_0 becomes larger, a_1 at the circular polarization becomes larger. The frequency at the circular polarization is 6.91GHz for b_0/a_0=0.97 and 4.24GHz for b_0/a_0=0.976. Fig. 4 shows the relative axial ratio bandwidth $\Delta f/f_0$. $\Delta f/f_0$ becomes wider as b_0/a_0 becomes larger.

Fig. 5 shows the electric field radiation patterns at the circular polarization. In the case of b_0/a_0=0.97, the axial ratio beamwidth (A.R. <3dB) are 115° and 113° in the xz- and yz-plane, respectively.

Fig. 6 shows the electric field distributions in the antenna apertures. At the circular polarization in Fig. 6(a), the travelling waves are observed. While, as the axial ratio deteriorates, the standing wave becomes dominant.

Table 1 compares the characteristics of elliptical ring antenna and ellptical patch antennas with same semimajor axis. The latter is calculated by using the method in the reference [1]. The frequency at the circular polarization in the ring antenna is considerably lower than that in the patch antenna. Hence, if both antennas are adjusted to have the same frequency at the circular polarization, the ring antenna will have a smaller size and a wider axial ratio bandwidth compared with the patch antenna.

4. Conclusion

The elliptical ring microstrip antenna has been analyzed numerically and its characteristics has been examined. From the numerical results it is found that the elliptical ring antenna has the wider axial ratio bandwidth than the elliptical patch antenna. The axial ratio bandwidth can be further increased by increasing b_0/a_0. Since the size of antenna becomes smaller in this case, however, the input impedance characteristics of this antenna will deteriorate. Therefore the input impedance characteristics of this antenna must be studied in the future.

Now we obtain the optimum axial ratio 0.48dB for the experimental model of antenna. The comparison between the theoretical results and the measured ones will be the future subject.

References

[1] L.C.Shen: "The elliptical microstrip antenna with circular polarization", IEEE Trans., AP-29, 1, pp.90-94, Jan. 1981.

[2] L.C.Shen: "Analysis of a circular-disc printed-circuit antenna", Proc. IEE, 126, 12, pp.1220-1222, Dec. 1979.

[3] K.Yasuura: "Numerical analysis of boundary value problem", in Modern Analysis of Electromagnetic Field, Chap.2, edited by T.Iijima, IECE, Aug. 1979.

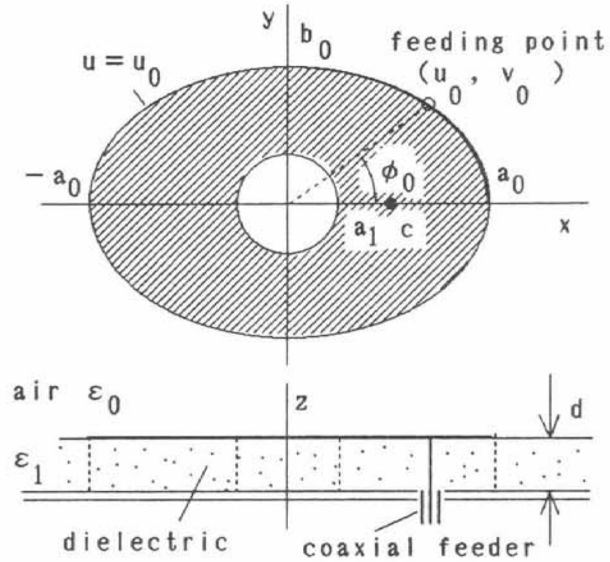

Fig.1 An elliptical ring microstrip antenna

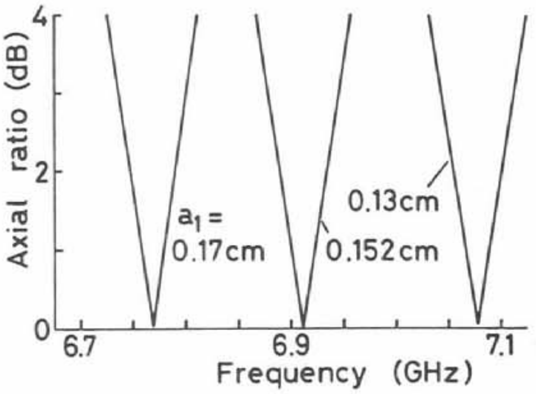

Fig.2 Optimum axial ratio
a_1=0.22cm

a_0=0.752cm, $\varepsilon_r=\varepsilon_1/\varepsilon_0$=2.15, ϕ_0=45°, d=0.764mm

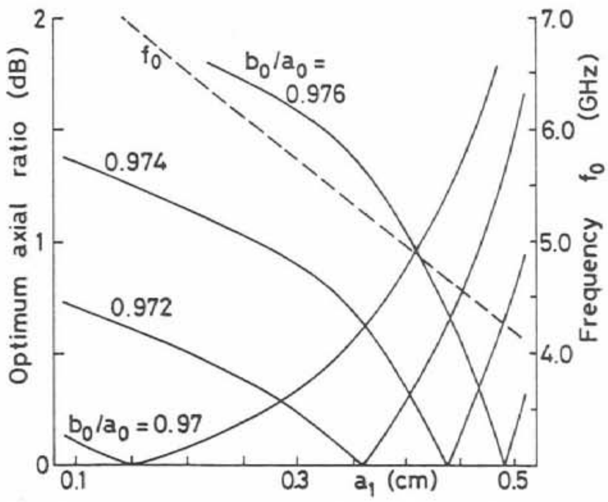

Fig.3 Optimum axial ratio and its frequency

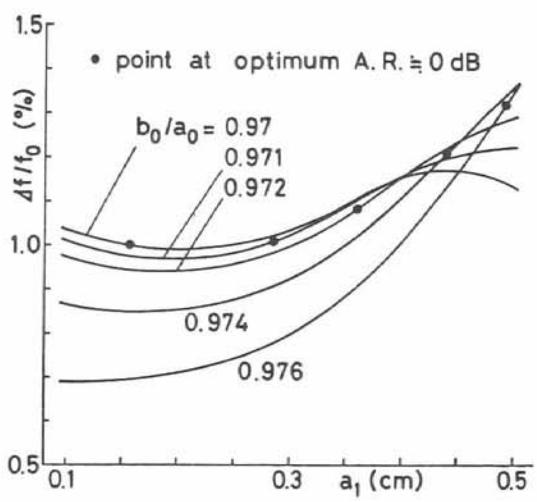

Fig.4 Axial ratio bandwidth
(Axial ratio ≦ 3dB)

Table 1 Comparison of the characteristics
of elliptical ring and patch antennas

	patch antenna	ring antenna	
a_0	0.752cm	0.752cm	0.752cm
b_0/a_0	0.97	0.97	0.972
a_1	——	0.152cm	0.358cm
f_0 at A.R.=0dB	7.4GHz	6.91GHz	5.24GHz
$\Delta f/f_0$(A.R.≦3dB)	1.1%	1.0%	1.06%

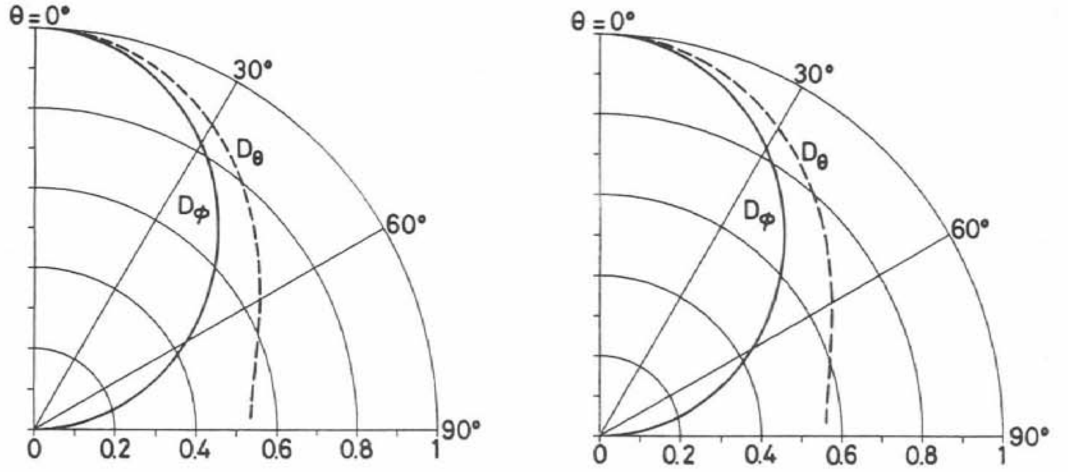

xz-plane (ϕ=0°)   yz-plane (ϕ=90°)

Fig. 5 Electric field radiation patterns b_0/a_0=0.97, a_1=0.152cm, frequency=6.91GHz

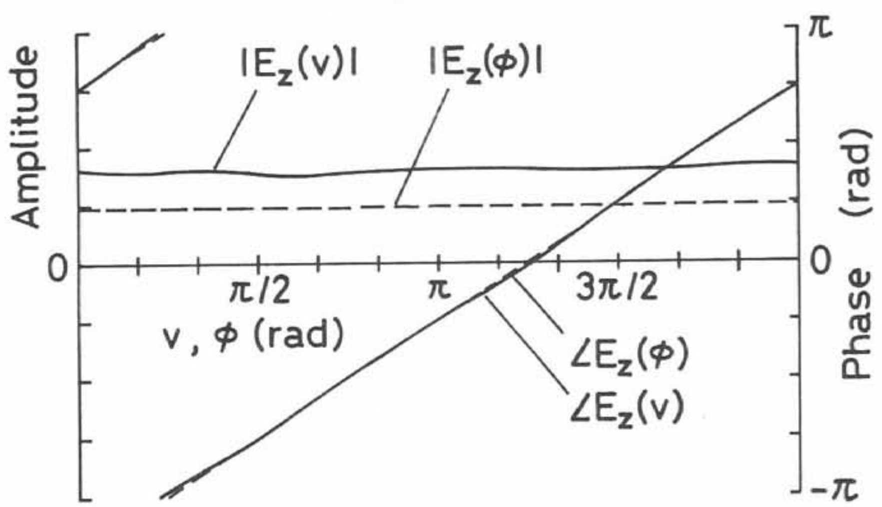

(a) frequency=6.91GHz

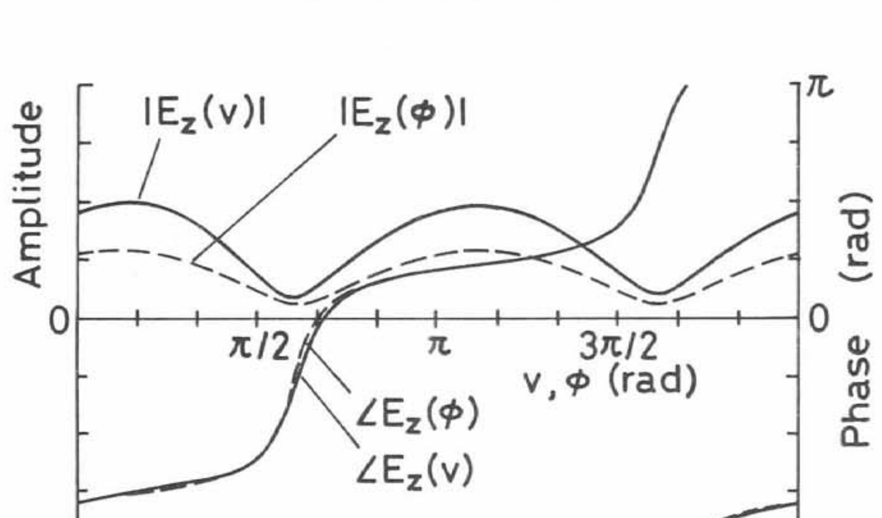

(b) frequency=6.75GHz

Fig. 6 Electric field distributions at apertures b_0/a_0=0.97, a_1=0.152cm